LA-UR -76-2285

Conf-761006--10

TITLE: AN ALL EPITAXIAL SILICON DIODE HEAVY ION DETECTOR

AUTHOR(S): C. R. Gruhn, P. D. Goldstone, and Nelson Jarmie

SUBMITTED TO: 1976 Nuclear Science Symposium to be published in the IEEE Proceedings

MASTER

los alamos
scientific laboratory
of the University of California
LOS ALAMOS, NEW MEXICO 87545

Form No. 836
St. No. 2629
1/75

UNITED STATES
ENERGY RESEARCH AND
DEVELOPMENT ADMINISTRATION
CONTRACT W-7405-ENG. 36

AN ALL EPITAXIAL SILICON DIODE HEAVY ION DETECTOR†

C. R. Gruhn, P. D. Goldstone, and Nelson Jarmie*

ABSTRACT

An all epitaxial silicon diode (ESD) heavy ion detector has been designed, fabricated, and tested. The active area of the detector is 5 cm^2 and has a total thickness of 50 μ. The response of the detector has been studied with fission fragments, alpha particles, oxygen ions, and sulfur ions. A number of advantages in terms of both fabrication and performance are discussed.

INTRODUCTION

A large area (5 cm^2), all epitaxial silicon diode (ESD) heavy ion detector has been designed, fabricated, and tested. The design offers advantages due to the low resistivity (33 Ω-cm) of the epitaxial layers and the economics of fabrication. The design is compatible with lectro-thinning processes[1] and has been successfully thinned with areas up to 5 cm^2.

The response of the ESD detector has been measured using several sources of heavy ions. The response to fission fragments was measured. Oxygen ions from the reaction ^{197}Au (^{16}O, ^{16}O) for energies between 13 and 54 MeV were used to probe the response of the detector for various detector biases. The charge defect has an unusual bias dependence with implications of an interesting charge transport process. The detector has a most favorable response at lowest biases. Sulfur ions (92.5 MeV) having angles of incidence both normal and 45° with respect to the junction give results which confirm the oxygen ion data. Resolutions limited by Nyquist noise and the high capacitance of the detector were observed.

DESIGN

The purpose of the ESD detector design was to achieve a large area, economical, relatively radiation resistant heavy ion detector. As indicated in the detector response section, other design features were discovered which deserve optimization in any future ESD detector design. No optimization of the design is attempted in this paper.

The basic ESD detector design is seen in Fig. 1. The detector consists of an epitaxial diode having a 77 Ω-cm (13.6 μm) p-type epitaxial layer upon a 33 Ω-cm (34. μm) n-type epitaxial layer. The substrate of the epitaxial layers is 0.01 Ω-cm (200 μm thick) n^+-type and is 2-in. in diameter.

The fabrication is relatively simple. A 1-1/4-in. diameter mesa is etched on the wafer such that the junction is exposed at the rim. This serves as means of pinching off the surface field in the n-type region. A gold contact, 1-1/8-in. in diameter, 200°A thick, was evaporated upon the p-type mesa. The signal was taken from this contact. For the tests in this paper the substrate under the mesa was not removed. However, other devices identical in design where the substrate under the mesa has been removed using the electro-thinning technique of R. L. Meek[1] have been constructed.

†Work performed under the auspices of the U. S. Energy Research and Development Administration, Contract W-7405-ENG. 36.

*University of California, Los Alamos Scientific Laboratory, P. O. Box 1663, Los Alamos, NM 87545.

The cost of the ESD detector was primarily labor. The total cost in materials was approximately $30.00. The labor was 4 hours for a not so experienced technician (CRG).

ESD Detector Response

The electronic chain in these measurements consisted of the diode, an Ortec 125 charge integrating preamplifier, a TC-205A (Tennelec) shaping amplifier, and a pulse-height analyzer. The electronics and charge measurements were calibrated using an Ortec 448 precision pulser. The LASL tandem Van de Graaff was used to produce the heavy ions for the detector response measurements.

In Fig. 2 we show the response of the detector to fission fragments from the reaction ^{244}Pu + d (15 MeV). The data were taken using a 3/4-in. diameter collimator.

The response of the detector to oxygen ions from the reaction ^{197}Au (^{16}O, ^{16}O) was studied as a function of incident oxygen energy and detector bias. In Fig. 3 we show the response of the detector to the oxygen ions from this reaction. The detector for this particular spectrum had a bias of 9 V. The depletion width (∿ 11 μm) is only a fraction of the range of either the oxygen ions (∿ 39 μm) or the alpha particles (∿ 28 μm). The filter time constant of the shaping amplifier was set at 0.5 μsec. Upon checking with the precision pulser it was determined that most of the charge (within 2%) was being collected. It was also observed in this check that the charge collection efficiency improved with decreasing bias. This was contrary to any expectation based upon previous experience.[2]

Because of this latter statement, the following studies were made of the electronics:

1. The same bias dependence and efficiencies were obtained for 0.5, 2.0, and 8.0 μsec shaping time constants.

2. The same efficiencies were measured when a 5000 pf capacitance was placed in parallel with the ESD.

3. The same efficiencies were measured when 50 Ω was placed in series to the preamplifier.

4. The combination of checks 2 and 3 gave the same result.

The conclusion was that the effect was not likely an artifact of the electronics, but rather a physical feature of the charge transport.

At this point it was decided to study the charge collection efficiency in detail as a function of the oxygen ion energy (range) and ESD bias. The results of these measurements are shown in Fig. 4. The important features of the data are:

1. For ranges long compared to the junction depth, the charge collection efficiency is greatest for smaller depletion widths.

2. For ranges short compared to the junction depth, the charge collection efficiency is low, and increases with depletion width.

The crossover at the junction between features 1 and 2 is taken as additional evidence that the effect is not an electronic artifact.

Feature 1 is new and cannot be reconciled with any known gain mechanism (transistor or avalanche multiplication).

The charge collection efficiency of the ESD was checked further using 92.5 MeV sulfur ions as a function of bias and angle of incidence for the ion. The range of these particles in silicon is 37 μm. The angles of incidence for the ions were 90.0 and 45.0 degrees to the plane of the junction. The results are shown in Fig. 5. The main features of this data are:

1. The oxygen ion results are confirmed for normal incidence.

2. For 45 degree incident angle the efficiency is less and the bias dependence is less strong than for normal incidence.

The second feature in this result is taken as further evidence that the effect is not an electronic effect.

THEORY

A charge transport model is proposed which we believe explains the major features of the data in the previous section. The model is called "Dipole Induced Charge Transport." The charge transport is space charge assisted (SCA). The charge transport is exactly that which one would associate with the so-called "Long diode" i.e., a diode having undepleted material on each side of the junction with a long recombination lifetime. A second analogy can be found in the charge transport of a "step recovery" diode. The difference between our case and this latter analogy is that the undepleted material is minimized and has a short recombination lifetime for the "step recovery" diode.

The charge transport is governed by the following:

The real currents

$$\text{electrons,}\quad J_n = en\mu_n E + eD_n \frac{\partial n}{\partial x} \tag{1}$$

$$\text{holes,}\quad J_p = ep\mu_p E - eD_p \frac{\partial p}{\partial x} \tag{2}$$

The transport involves both drift and diffusion as given in Eqs. 1 and 2.

The continuity equations

$$\text{electrons,}\quad \frac{\partial n}{\partial t} = -\frac{n-n_o}{\tau_n} + \frac{1}{e}\frac{\partial J_n}{\partial x} \tag{3}$$

$$\text{holes,}\quad \frac{\partial p}{\partial t} = -\frac{p-p_o}{\tau_p} - \frac{1}{e}\frac{\partial J_p}{\partial x}$$

Poisson's equation

$$\frac{\varepsilon}{e}\left(\frac{\partial E}{\partial X}\right) = (p-p_o) - (n-n_o) \tag{4}$$

From Maxwell's equations it can be shown that the sum of the real currents and the displacement current is independent of position.

$$J(t) = J_p(x,t) + J_n(x,t) + \varepsilon \frac{\partial E(x,t)}{\partial t} \tag{5}$$

It is assumed that the voltage across the ESD is constant, that is:

$$\int_{ESD} E(x,t)\,\partial x = \text{constant} \tag{6}$$

A numerical analysis and solution to these expressions for this particular transport problem is to be published elsewhere.[4] A schematic solution is given in Fig. 6.

A solution of Poisson's equation with n and p equal to zero gives the initial electric field profile. The ionizing particle produces a plasma of approximately uniform density over a distance of the range of the particle. At this time the charge transport is one dominated by drift in the depletion region and diffusion in the undepleted regions. The plasma polarizes with the electrons and holes drifting to the edge of depletion region. Their space charge is such as to diminish the electric field in the depleted region. This transport continues until sufficient charge has accumulated at the edge of the depletion to have reduced the field in the depleted region to nearly zero.

Now because the voltage across the entire device is held constant the integral of the electric field in the depletion region which is reduced by the field of the space charge must appear in equal amount in the undepleted region. This is expected to occur in a time of the order of 10^{-10} sec for the ESD design. The charge transport in the undepleted region is now a drift dominated transport due to the space charge field (dipole). The charge transport in the depletion region is dominated by diffusion due to the superposition of the dipole field on the original field. The transport is "blocked" between the poles of the dipole for a diffusion time which depends upon the depletion width. The charge in the plasma is cleared from the undepleted regions by a drift transport over a time duration of approximately 3×10^{-9} sec for the ESD design. Some of the charge from the undepleted regions drifts to the blocked region and is stored for approximately a diffusion time ($\sim 10^{-7}$ sec). It is mostly this stored charge in the "blocked" region (because of the long storage time) which experiences recombination and contributes to the inefficiency of the charge measurement. In effect, the induced dipole field of the space charge has contributed to a space charge assisted (SCA) transport.

Qualitatively one can now calculate the charge collection efficiency as a function of bias across the ESD. We make the assumption that the range, R, is large compared to either the junction depth, X, or depletion width, W.

The measured charge, Q_m, as compared with the initial charge, Q_L, in the plasma is given by:

$$\xi = \frac{Q_m}{Q_L} = .75 - .5\frac{W}{R} + (.25 + .5\frac{W}{R})\exp(-3\tau_p/\tau_R) \tag{7}$$

where τ_R = the recombination lifetime

and τ_D = the $\frac{W^2}{2D_A}$, the diffusion time

and $W = 3.67\ V^{1/2}$ μm for this ESD design.

The only free parameter in this expression is the recombination lifetime. Using the data at 20 V in Fig. 5 we find a recombination lifetime of 2×10^{-6} sec.

The model qualitatively accounts for all the features of the data. The data in Fig. 4 are accounted for as follows:

1. For ranges long compared to the junction depth, the charge collection efficiency is greatest for smaller depletion widths because the charge storage time in the blocked region (depleted region) is least for the smaller depletion widths and therefore there is less recombination for lower biases.

2. For ranges short compared to the junction depth, the charge collection efficiency is low, and increases with depletion width because the amount of charge stored and the storage time is least for the widest depletion widths and therefore there is less recombination for higher biases.

The data in Fig. 5 are accounted for as follows:

1. The confirmation of the oxygen results carries the same explanation as (1) above.

2. For 45 degrees incident angle, the efficiency is less and the bias dependence is less strong than for normal incidence. In this case some of the charge transport is off the edge of the dipole field. This results in a superposition charge transport having effective ranges long and short compared to the junction depth. See Fig. 4. The result being in a net cancellation of the bias dependence.

CHARGE DEFECT

In general, the net charge defect in the detection of heavy ions is due to a superposition of effects. Some of these effects are:

1. Dead layers due to electrodes.

2. Non-ionizing collision energy losses.

3. Recombination.

For that portion of the defect due to recombination, it is interesting to make a comparison between the ESD design and the commonly used surface barrier detector. If one assumes an ESD operating at low bias and a fully depleted surface barrier detector each having equivalent recombination lifetimes and resistivities, the ESD in principle will lose one-quarter as much charge by recombination as the surface barrier detector. The reason for this is because in the case of the surface barrier all of the charge is immediately blocked for a plasma decay time and in the case of the ESD only about one-quarter of the charge is blocked for a diffusion time. In practice, however, since the plasma decay times are significantly shorter than the diffusion, the net recombination losses are about the same.

SUMMARY

The ESD detector design offers the following advantages:

1. An economical detector.

2. Relatively large areas are possible. Epitaxial wafer areas at the present are ≤ 75 cm^2.

3. Lower resistivity designs are possible even when the depletion width is small compared to the range of the particles detected.

4. The lower resistivity designs are expected to result in a longer radiation lifetime.

5. The detection of ionization is one involving a space charge assisted transport (not space charge limited).

ACKNOWLEDGEMENTS

The authors are appreciative of discussions with V. Radeka, BNL, R. Fair, BTL, C. Maggiore, S. Depp, P. W. Keaton, and J. Narud, LASL. We wish to thank the able assistance of the operators of the LASL tanden Van de Graaff and P. Kelley for the typing of this manuscript.

REFERENCES

1. R. L. Meek, W. M. Gibson, and R. H. Braun, Preparation of Supported, Large-Area, Uniformly Thin Silicon Films for Particle-Channeling Studies, Nucl. Instr. Meth. 94, 435-442, June 1971.

2. E. Konecky and K. Hetwer, Response of Semiconductor Surface Barrier Detectors to Fission Fragments, Nucl. Instr. Meth. 36, 61-72, September 1965.

3. C. R. Gruhn and C. Maggiore, Dipole Induced Transport (to be published).

FIGURE CAPTIONS

Fig. 1. Design of an epitaxial silicon diode (ESD) detector.

Fig. 2. ESD response to fission fragments.

Fig. 3. ESD response to oxygen ions.

Fig. 4. Charge collection efficiency as a function of oxygen ion range and ESD bias.

Fig. 5. Charge collection efficiency for 92.5 MeV sulfur ions as a function of ESD bias.

Fig. 6. Dipole induced transport, schematic model.

EPITAXIAL SILICON DIODE (ESD)

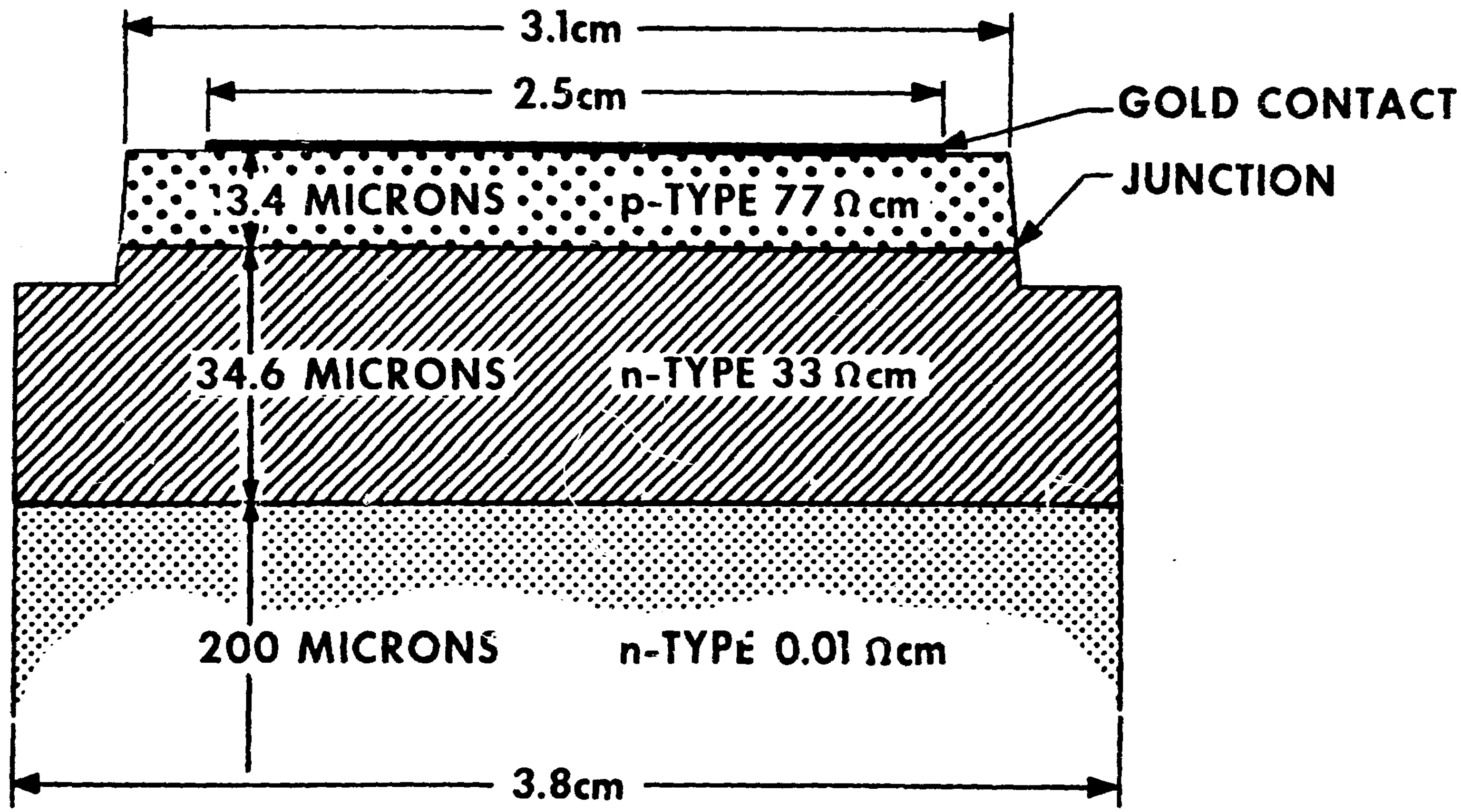

Fig. 1

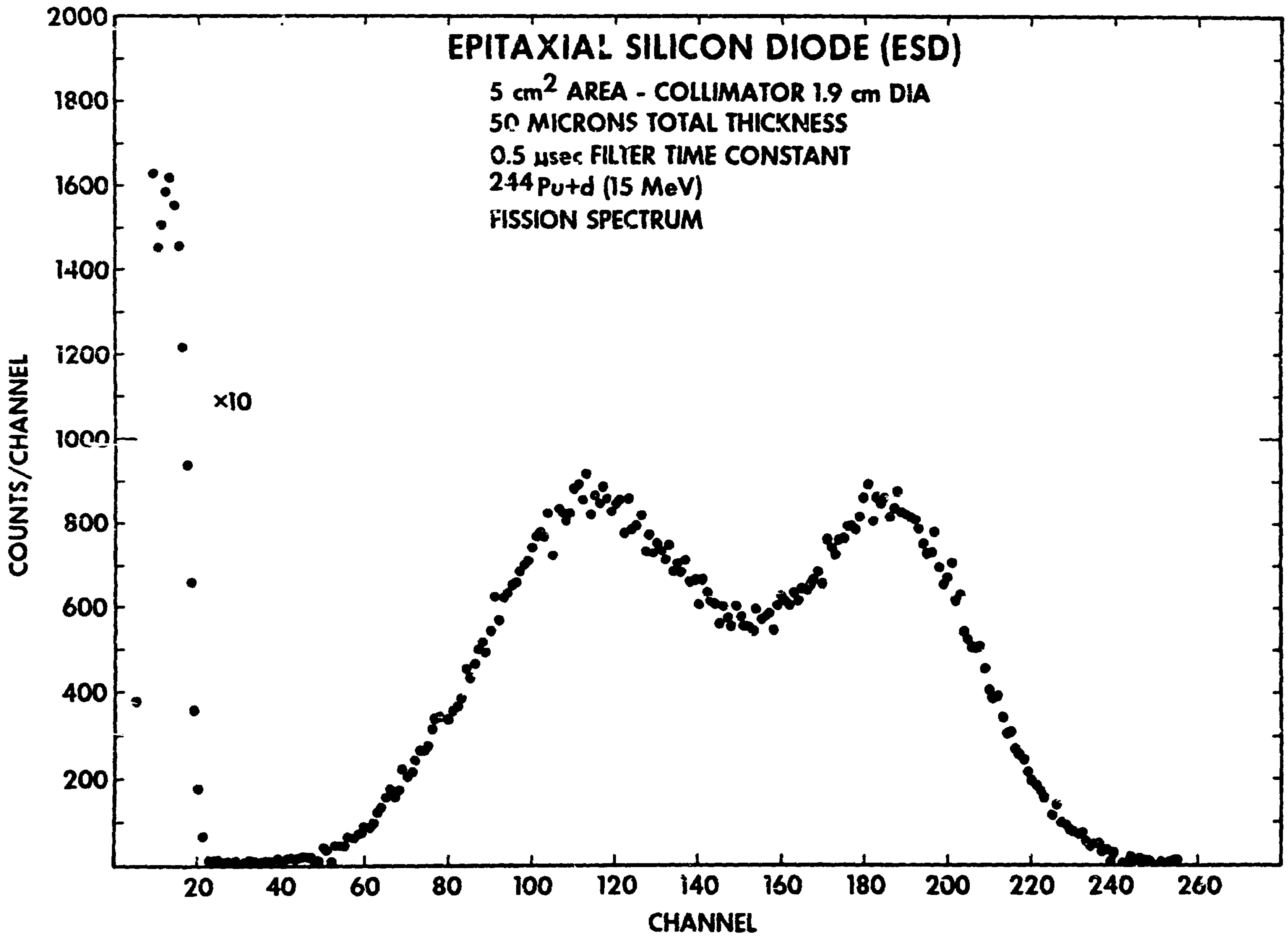

EPITAXIAL SILICON DIODE (ESD)
5 cm2 AREA - COLLIMATOR 1.9 cm DIA
50 MICRONS TOTAL THICKNESS
0.5 μsec FILTER TIME CONSTANT
244Pu+d (15 MeV)
FISSION SPECTRUM
×10
COUNTS/CHANNEL
CHANNEL
2000
1800
1600
1400
1200
1000
800
600
400
200
20
40
60
80
100
120
140
160
180
200
220
240
260

Fig. 2

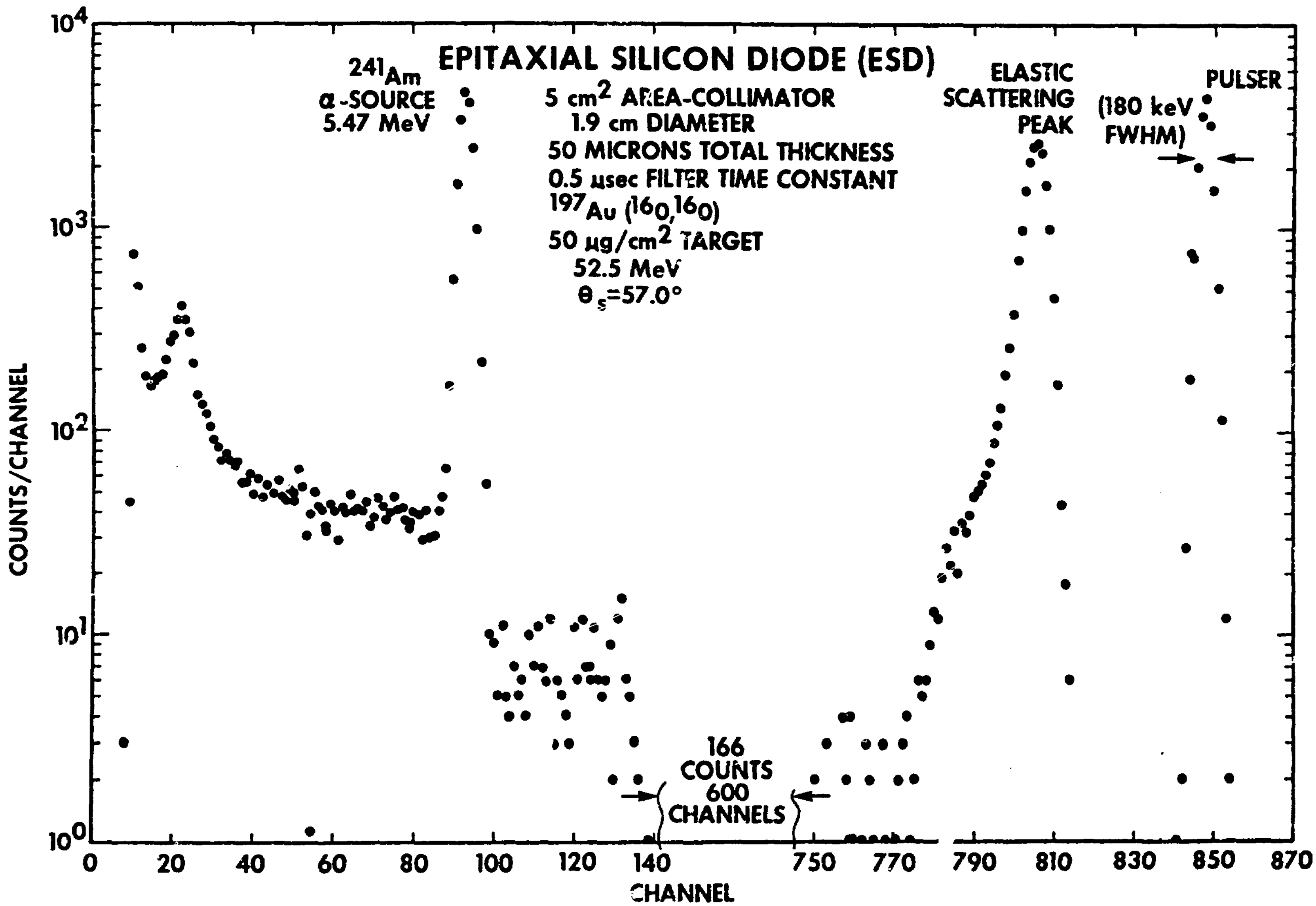

EPITAXIAL SILICON DIODE (ESD)
241Am
α-SOURCE
5.47 MeV
5 cm2 AREA-COLLIMATOR
1.9 cm DIAMETER
50 MICRONS TOTAL THICKNESS
0.5 μsec FILTER TIME CONSTANT
197Au (16O,16O)
50 μg/cm2 TARGET
52.5 MeV
θs=57.0°
ELASTIC SCATTERING PEAK
PULSER
(180 keV FWHM)
166 COUNTS
600 CHANNELS
COUNTS/CHANNEL
CHANNEL

Fig. 3

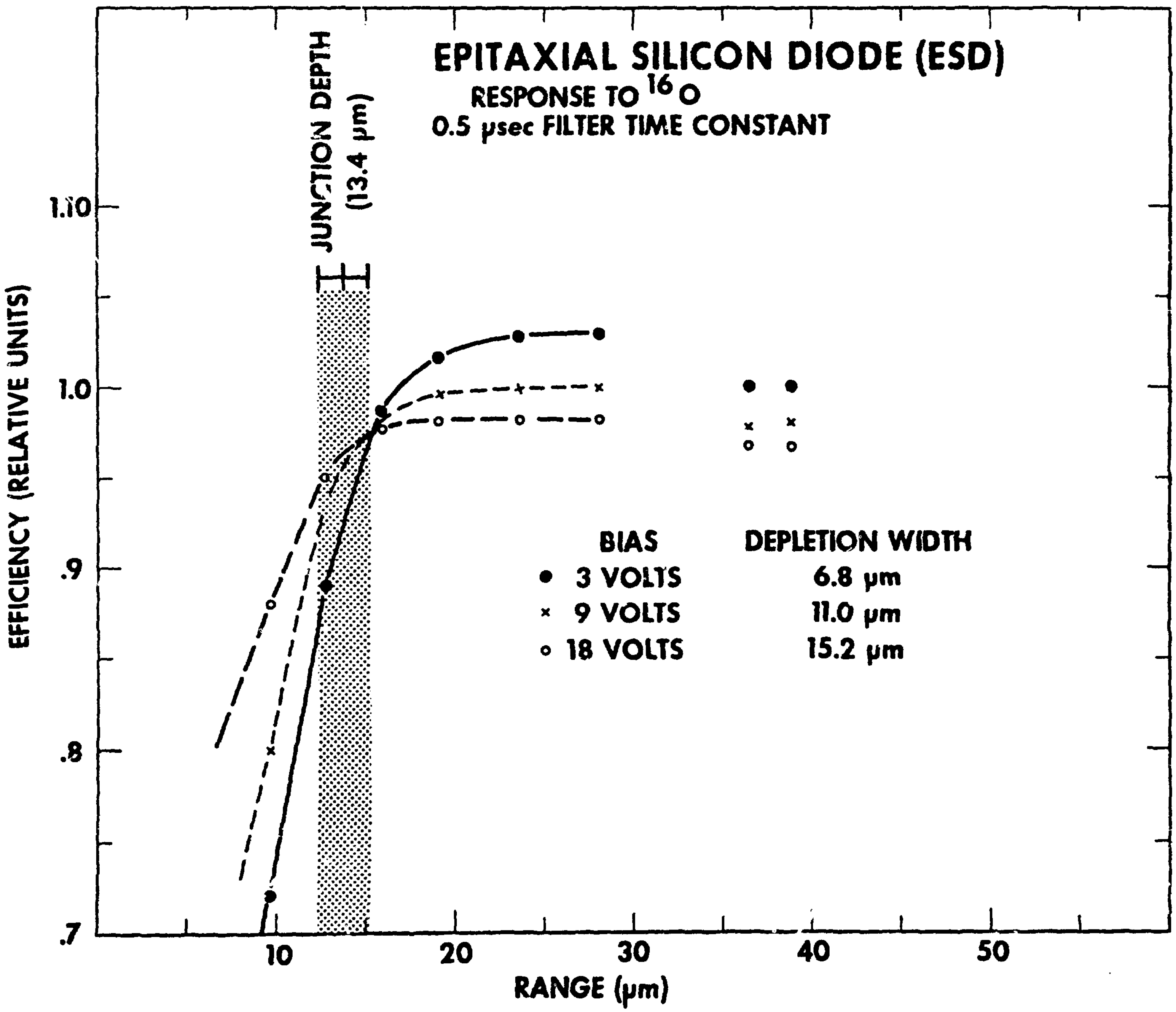
EPITAXIAL SILICON DIODE (ESD)
RESPONSE TO ^{16}O
0.5 μsec FILTER TIME CONSTANT
JUNCTION DEPTH
(13.4 μm)
EFFICIENCY (RELATIVE UNITS)
1.10
1.0
.9
.8
.7
10
20
30
40
50
RANGE (μm)
BIAS
DEPLETION WIDTH
3 VOLTS
6.8 μm
9 VOLTS
11.0 μm
18 VOLTS
15.2 μm

Fig. 4

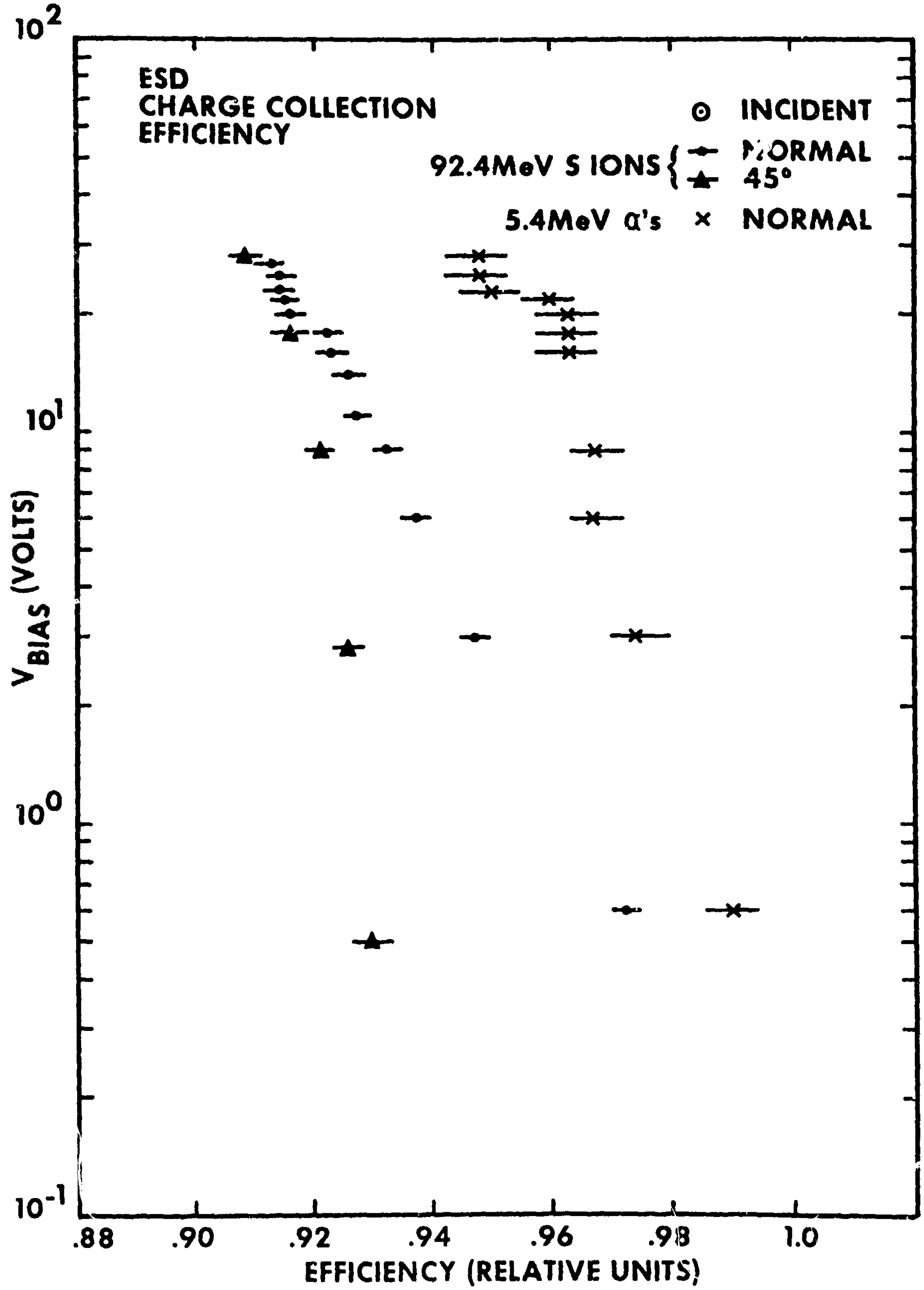
ESD
CHARGE COLLECTION
EFFICIENCY
INCIDENT
92.4MeV S IONS
NORMAL
45°
5.4MeV α's
NORMAL
10^2
10^1
10^0
10^{-1}
V_{BIAS} (VOLTS)
.88
.90
.92
.94
.96
.98
1.0
EFFICIENCY (RELATIVE UNITS)

Fig. 5

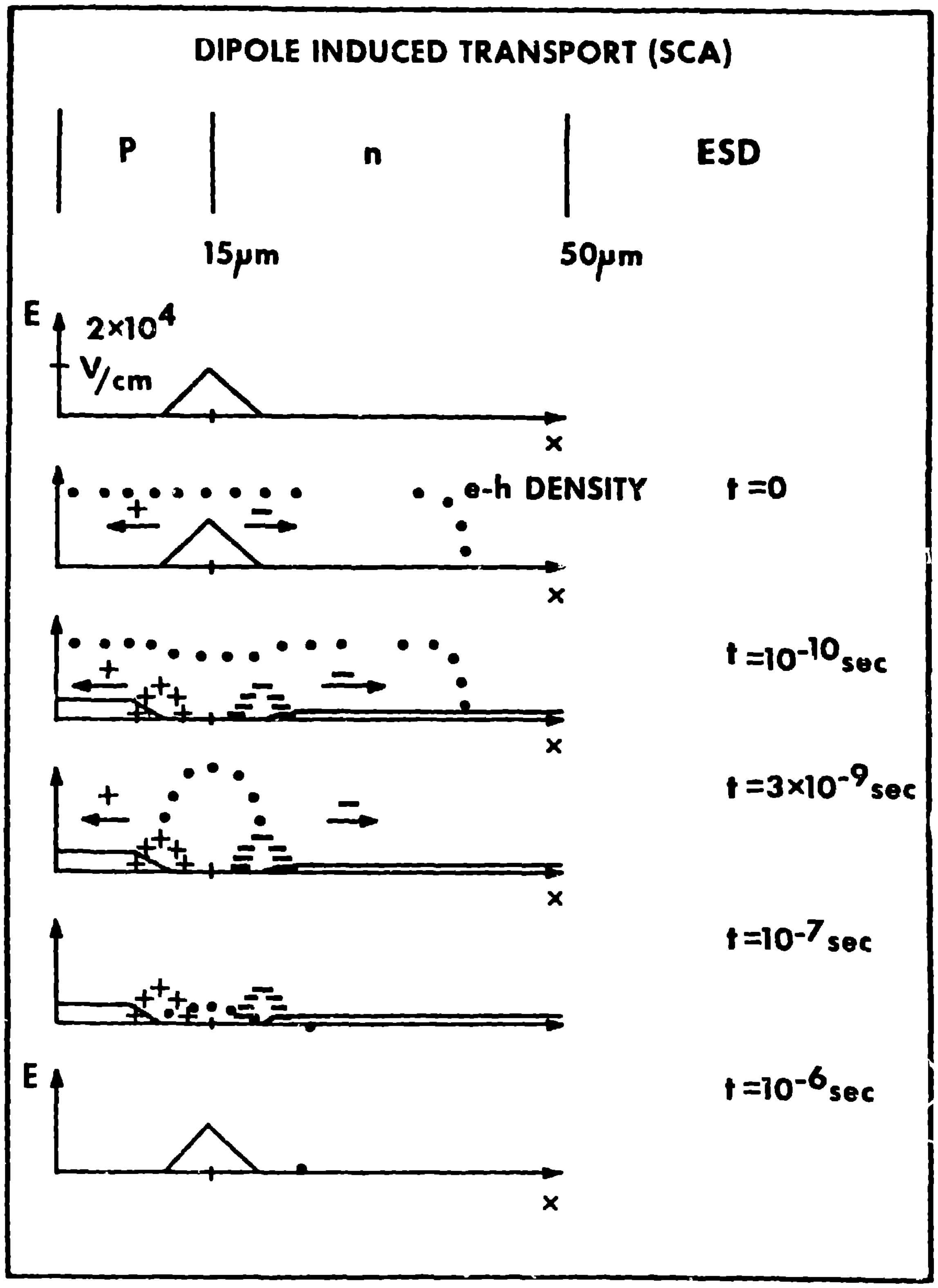
DIPOLE INDUCED TRANSPORT (SCA)
P
n
ESD
15μm
50μm
E
2×10^4 V/cm
x
e-h DENSITY
t =0
t =10^-10 sec
t =3×10^-9 sec
t =10^-7 sec
t =10^-6 sec

Fig. 6